

# Diprotonated [28]Hexaphyrins(1.1.1.1.1.1): Triangular Antiaromatic Macrocycles\*\*

Shin-ichiro Ishida, Tomohiro Higashino, Shigeki Mori, Hirotaka Mori, Naoki Aratani, Takayuki Tanaka, Jong Min Lim, Dongho Kim,\* and Atsuhiko Osuka\*

**Abstract:** Protonation of *meso*-aryl [28]hexaphyrins(1.1.1.1.1.1) triggered conformational changes. Whereas protonation with trifluoroacetic acid led to the formation of monoprotonated Möbius aromatic species, protonation with methanesulfonic acid led to the formation of diprotonated triangular antiaromatic species. A peripherally hexaphenylated [28]hexaphyrin was rationally designed and prepared to undergo diprotonation to favorably afford a triangular-shaped antiaromatic species.

Expanded porphyrins are often structurally flexible and display diverse molecular shapes, which often dictate their electronic properties.<sup>[1]</sup> Regular hexaphyrins(1.1.1.1.1.1) that consist of six pyrrole rings arranged in alternate orientations separated by the *meso* carbon atoms have been shown to adopt various conformations, such as rectangular,<sup>[2]</sup> dumb-bell,<sup>[3]</sup> figure-of-eight,<sup>[4]</sup> and twisted Möbius strip-like shapes,<sup>[5]</sup> depending on the *meso* and peripheral substituents, intramolecular hydrogen bonding, stabilization induced by aromaticity, and the nature of the coordinated metal. A triangular shape is also a possible conformation for hexaphyrins, but has only been observed for a protonated *meso*-hexaphenyl [26]hexaphyrin(1.1.1.1.1.1).<sup>[6]</sup> Intriguingly, this hexaphyrin is extremely unstable in its free base form because of rapid oxidative decomposition. Herein, we report protonation-triggered conformational changes of [28]hexaphyrins(1.1.1.1.1.1) that provide a mono-protonated Möbius aromatic species upon treatment with trifluoroacetic acid (TFA) and a diprotonated triangular Hückel antiaromatic

species in the presence of methanesulfonic acid (MSA). The latter process constitutes a rare, but reliable method for the synthesis of triangular antiaromatic hexaphyrins (Figure 1).<sup>[7,8]</sup>

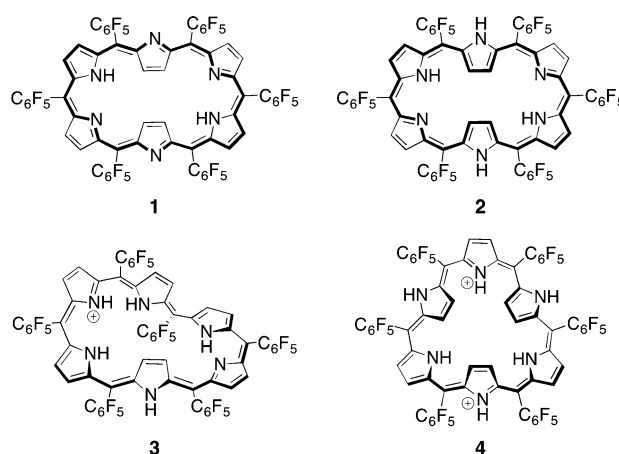


**Figure 1.** Structures of hexakis(pentafluorophenyl) [26]hexaphyrin **1**, its [28]hexaphyrin congener **2**, and monoprotonated and diprotonated [28]hexaphyrins **3** and **4**.

[28]Hexaphyrin **2**, which is prepared by the reduction of [26]hexaphyrin **1** with NaBH<sub>4</sub>, is known to exist as a dynamic conformational mixture of twisted Möbius aromatic and planar Hückel antiaromatic species at room temperature.<sup>[5c]</sup> Encouraged by the recently described protonation-triggered formation of Möbius aromatic species from [32]heptaphyrins and [36]octaphyrin,<sup>[9]</sup> we examined the protonation of **2**. The absorption spectrum of neutral **2** in CH<sub>2</sub>Cl<sub>2</sub> exhibits a Soret band at 591 nm and a Q band at 762 nm, reflecting a predominance of the Möbius conformers in the conformational mixture. Addition of TFA to this solution caused a red shift of the Soret-like band from 591 nm to 621 nm with clear intensification and red shifts of the Q-like bands to 847 and 945 nm (Figure 2a). These spectral changes can be interpreted in terms of a shift from the above-mentioned dynamic conformational mixture to a distribution that is dominated by the monoprotonated Möbius aromatic species **3**. The <sup>1</sup>H NMR spectrum of **3** in CDCl<sub>3</sub> exhibits signals at  $\delta$  = 8.28 and 7.80 ppm, which correspond to the outer  $\beta$  protons, and a signal at  $\delta$  = 0.02 ppm, which is due to the inner  $\beta$  protons, at room temperature (see the Supporting Information). These spectral patterns were interpreted in terms of a fast conformational exchange between the Möbius aromatic species and the rectangular Hückel antiaromatic species, which leads

[\*] S. Ishida, T. Higashino, Dr. S. Mori, H. Mori, Dr. N. Aratani, Dr. T. Tanaka, Prof. Dr. A. Osuka  
Department of Chemistry, Graduate School of Science  
Kyoto University  
Sakyo-ku, Kyoto, 606-8502 (Japan)  
E-mail: osuka@kuchem.kyoto-u.ac.jp

Dr. J. M. Lim, Prof. Dr. D. Kim  
Spectroscopy Laboratory for Functional  $\pi$ -Electronic Systems and  
Department of Chemistry  
Yonsei University  
Seoul 120-749 (Korea)  
E-mail: dongho@yonsei.ac.kr

[\*\*] The work at Kyoto was supported by a Grant-in-Aid (25220802 (S)) for Scientific Research from MEXT of Japan. T.H. and H.M. acknowledge JSPS Fellowships for Young Scientists. The work at Yonsei was supported by the Global Frontier R&D Program of the Center for Multiscale Energy System (2012-8-2081) of the National Research Foundation (NRF), which is funded by MEST of Korea, and AFSOR/AOARD (FA2386-09-4092).

Supporting information for this article is available on the WWW under <http://dx.doi.org/10.1002/anie.201400301>.

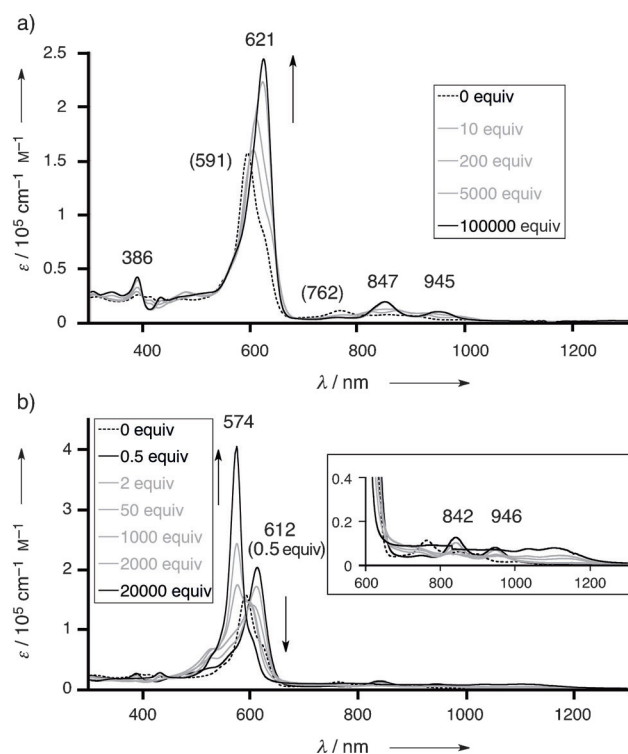


**Figure 2.** a, b) UV/Vis absorption spectral changes during titration of **2** with TFA (a) and MSA (b) in  $\text{CH}_2\text{Cl}_2$ .

to a symmetric  $^1\text{H}$  NMR spectral pattern that is due to the averaged conformational equilibrium and similar to that of **2**.<sup>[5c]</sup> The observed increase in diatropic ring current indicates a predominance of the Möbius aromatic conformers for **3**. In line with this interpretation, the  $^1\text{H}$  NMR spectrum of **3** at low temperature clearly indicated that only a single Möbius aromatic species is present (see the Supporting Information). Finally, the structure of **3** was revealed to be a twisted Möbius structure by X-ray diffraction analysis; the macrocyclic conjugation is connected through the nearly perpendicular pyrrole E and the inverted pyrrole F (Figure 3a). Importantly, further protonation of **3** could not be realized, even upon addition of a large excess of TFA.

Following these preliminary investigations, we examined the protonation of **2** with MSA, which is a stronger acid than TFA. Upon addition of up to 0.5 equivalents of MSA to a solution of **2** in  $\text{CH}_2\text{Cl}_2$ , formation of **3** was indicated by the appearance of a band at 612 nm in the absorption spectrum, but, upon further addition of MSA, a different species evolved as confirmed by a blue shift and further enhancement of the Soret-like band to 574 nm and replacement of the well-structured Q-like bands by a very broad absorption tail at up to 1200 nm (Figure 2b). These observations may simply be explained by considering further protonation of **3**, namely formation of diprotonated species **4**. Eventually, we obtained crystals of **4** by the slow diffusion of *n*-heptane into a solution of **2** in a mixture of  $\text{CHCl}_3$  and methanol in the presence of MSA. X-Ray analysis revealed that the structure of **4** is a triangle that consists of three corner pyrroles pointing inwards (A, C, and E) and three side pyrroles pointing outwards (B, D, and F), with a mean plane deviation of

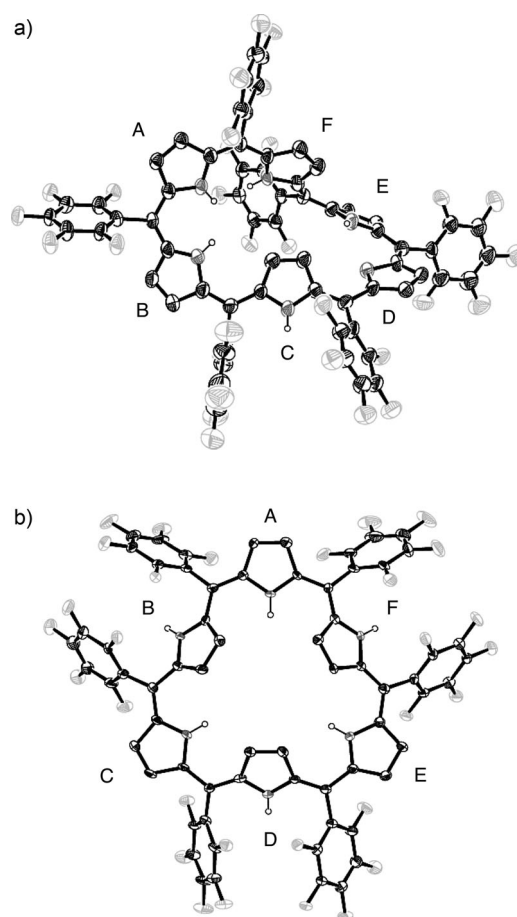
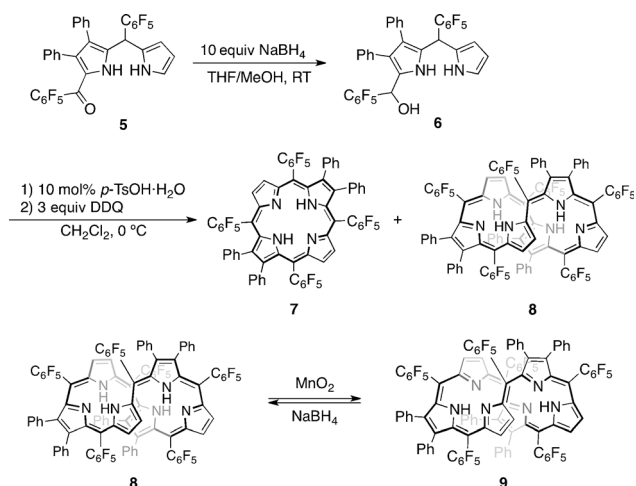


**Figure 3.** a, b) X-Ray crystal structures of **3** (a) and **4** (b). Thermal ellipsoids set at 30% probability. Counter anions and hydrogen atoms, except for those attached to nitrogen atoms, are omitted for clarity.

approximately 0.3 Å (Figure 3b). Therefore, hexaphyrin **4** was assigned as a Hückel antiaromatic diprotonated molecule owing to its planar structure and the  $\pi$ -conjugated system with 28 electrons. The disappearance of the Q-like bands and the broad absorption tail support its antiaromaticity.<sup>[1e,f,4c,10]</sup> The enhanced Soret-like band of **4** may be due to its high molecular symmetry (ca.  $D_{3h}$ ). The extended triangular conformation of **4** is likely favoured because of Coulombic repulsion between the two positive charges in the molecule.

Then, it occurred to us that rational peripheral modification of [28]hexaphyrins may render them more prone to adopting triangular geometries. Therefore, we designed 2,3,12,13,22,23-hexaphenyl [28]hexaphyrin **8**, which has an alternate arrangement of unsubstituted pyrroles and 3,4-diphenylpyrroles and may favor a  $C_3$ -symmetric triangular shape because of steric repulsion between the introduced phenyl groups. Synthesis of **8** was accomplished by self-condensation of monocarbinol **6**. Aroyl dipyrromethane precursor **5** was reduced with  $\text{NaBH}_4$  to provide **6**, which was then condensed in the presence of *para*-toluenesulfonic acid (*p*-TsOH) in  $\text{CH}_2\text{Cl}_2$ , followed by oxidation with 2,3-dichloro-5,6-dicyano-1,4-benzoquinone (DDQ). Purification by column chromatography on silica gel gave hexaphyrin **8** in 3% yield along with porphyrin **7**<sup>[11]</sup> in 11% yield (Scheme 1).



**Scheme 1.** Synthesis of [28]hexaphyrin **8** and [26]hexaphyrin **9**.

The structure of **8** was confirmed by X-ray diffraction analysis to be a figure-of-eight structure (see the Supporting Information). On the basis of the  $^1\text{H}$  NMR spectral data, [28]hexaphyrin **8** was assigned as a weakly antiaromatic species. In line with this, the absorption spectrum of **8** in  $\text{CH}_2\text{Cl}_2$  showed a broad band at 540 nm and very weak absorption in the near infrared region, which are characteristic signatures of antiaromatic porphyrinoids (see the Supporting Information). [28]Hexaphyrin **8** was quantitatively oxidized with  $\text{MnO}_2$  to afford [26]hexaphyrin **9**, the  $^1\text{H}$  NMR spectrum of which at  $-60^\circ\text{C}$  highlighted its weak but distinct aromaticity. The aromaticity of **9** was corroborated by its absorption spectrum in  $\text{CH}_2\text{Cl}_2$ , which displayed a sharp Soret band at 629 nm and Q-like bands at 800 and 902 nm (see the Supporting Information). [26]Hexaphyrin **9** could be easily reduced back to **8** under ambient conditions.

Protonation-induced conformational changes of **8** were examined by using TFA or MSA in  $\text{CH}_2\text{Cl}_2$ . The addition of TFA induced absorption spectral changes, such as the appearance of a remarkably sharp Soret band at 648 nm and Q-like bands at 861 and 981 nm (Figure 4a), which are quite similar to those observed for the titration of **2** with TFA; therefore, these changes were attributed to the formation of the monoprotonated Möbius aromatic species **10**. The  $^1\text{H}$  NMR spectrum of **10** in  $\text{CDCl}_3$  at  $-10^\circ\text{C}$  shows six signals that correspond to the pyrrolic  $\beta$  protons at  $\delta = 7.98$ , 7.69, 3.61, 2.95, 0.30, and  $-0.37$  ppm (Figure 5). These signals indicate that a single Möbius aromatic conformer is formed, and that the conformational dynamics are still slower than the  $^1\text{H}$  NMR time scale even at room temperature (see the Supporting Information), which is probably due to the steric congestion that is exerted by the peripheral phenyl substituents.<sup>[12]</sup> Titration of **8** with MSA initially produced **10**, as indicated by the appearance of a peak at 639 nm, but soon gave rise to diprotonated species **11** at the expense of **10** (Figure 4b). The absorption spectrum of the diprotonated species **11** shows a sharp peak at 619 nm, which is blue-shifted by 29 nm from that of **10**, and a weak long tail extended to approximately 1250 nm, which is similar to that observed for **4**. Finally, the structure of **11** was determined by single-crystal X-ray diffraction analysis (Figure 6). As expected, the pyr-

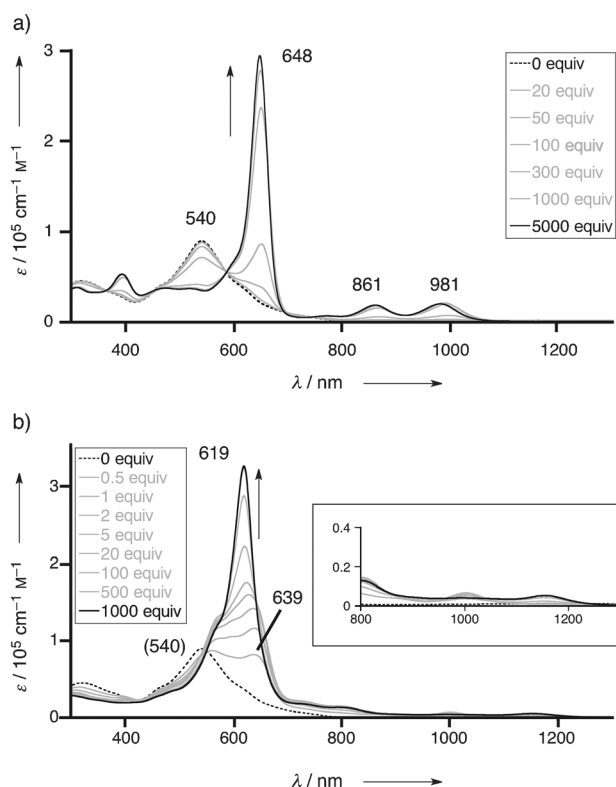


**Figure 4.** a, b) UV/Vis absorption spectral changes during titration of **8** with TFA (a) and MSA (b) in  $\text{CH}_2\text{Cl}_2$ .

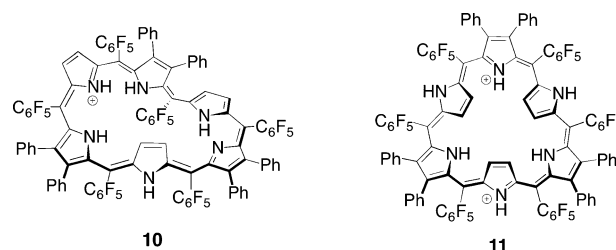


**Figure 5.** Monoprotonated [28]hexaphyrin **10** and diprotonated [28]hexaphyrin **11**.

roles and diphenylpyrroles are pointing outwards and inwards, respectively, to form a triangular conformation, in which steric congestion is apparently minimized. It is worthy to note that the amount of MSA needed for complete diprotonation of **8** is approximately 1000 equivalents, which is markedly smaller than the amount required for diprotonation of **2** (ca. 20000 equiv).

The excited-state dynamics of expanded porphyrins are sensitive to their molecular conformation and aromatic nature.<sup>[13]</sup> Thus, we examined the excited-state dynamics of [28]hexaphyrins by using femtosecond transient absorption spectroscopy. The singlet excited state of **8** shows a double exponential decay with ultrafast (0.4 ps, 75 %) and relatively long (5.1 ps, 25 %) time components. According to previous observations for highly distorted expanded porphyrins,<sup>[9]</sup> these very fast excited-state dynamics are mainly attributable to the acceleration of internal conversion processes in its figure-of-eight conformation. In contrast, the decay profiles of the ground-state bleaching recovery and the excited-state

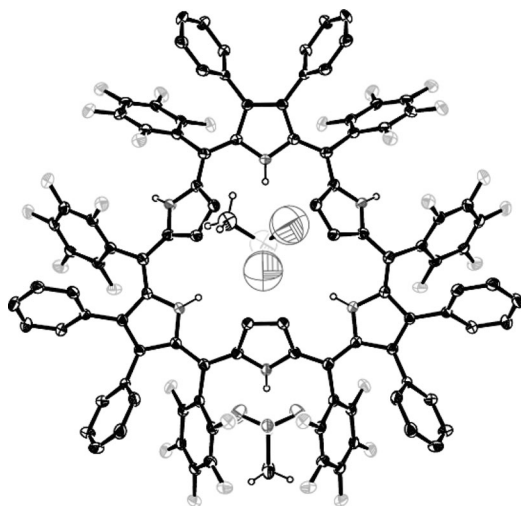


**Figure 6.** X-Ray crystal structure of **11** with counter anions. Thermal ellipsoids set at 30% probability. Solvents and hydrogen atoms, except for those that are attached to nitrogen atoms or part of methyl groups, are omitted for clarity.

absorption signals of monoprotonated [28]hexaphyrin **10** exhibited a relatively long decay time constant of 64 ps in THF in femtosecond transient absorption measurements. This feature is in good agreement with the Möbius aromatic nature of **10**. On the other hand, excited-state dynamics of diprotonated [28]hexaphyrin **11** revealed double-exponential decay profiles with ultrafast (0.7 ps, 80 %) and relatively long (8.9 ps, 20 %) time components. This spectroscopic feature is also characteristic of antiaromatic expanded porphyrins.<sup>[7,8]</sup> Furthermore, we observed fluorescence emission of the monoprotonated [28]hexaphyrin, whereas its neutral and diprotonated congeners are nonfluorescent. Therefore, the spectroscopic signatures that were observed for **8**, **10**, and **11** are all consistent with their assigned structures.

In summary, it has been shown that [28]hexaphyrin **2** is monoprotonated by TFA to afford the twisted Möbius aromatic species **3**, and that **2** is sequentially mono- and diprotonated by MSA to form **3** and the Hückel antiaromatic species **4** in a fully reversible fashion. 2,3,12,13,22,23-Hexaphenylated [28]hexaphyrin(1.1.1.1.1.1) **8** was rationally designed and prepared to undergo diprotonation to favorably afford a triangular-shaped antiaromatic species. For the diprotonated [28]hexaphyrins **4** and **11**, Coulombic repulsion between the two positive charges is most likely a key factor that encourages the triangular conformation with an electronically unfavorable antiaromatic character.<sup>[14]</sup> This work underlines the conformational flexibility of [28]hexaphyrins; conformational changes can be triggered by protonation. Importantly, this protonation strategy constitutes a reliable means to generate Möbius aromatic and antiaromatic expanded porphyrins.

Received: January 11, 2014

Published online: February 24, 2014

**Keywords:** antiaromaticity · hexaphyrin · Möbius aromaticity · protonation · triangular shape

- [1] a) J. L. Sessler, D. Seidel, *Angew. Chem.* **2003**, *115*, 5292; *Angew. Chem. Int. Ed.* **2003**, *42*, 5134; b) M. Stępień, N. Sprutta, L. Latos-Grażyński, *Angew. Chem.* **2011**, *123*, 4376; *Angew. Chem. Int. Ed.* **2011**, *50*, 4288; c) T. K. Chandrashekar, S. Venkatraman, *Acc. Chem. Res.* **2003**, *36*, 676; d) S. Shimizu, A. Osuka, *Eur. J. Inorg. Chem.* **2006**, 1319; e) S. Saito, A. Osuka, *Angew. Chem.* **2011**, *123*, 4432; *Angew. Chem. Int. Ed.* **2011**, *50*, 4342; f) A. Osuka, S. Saito, *Chem. Commun.* **2011**, 47, 4330; g) M. Stępień, L. Latos-Grażyński, N. Sprutta, P. Chwalisz, L. Szterenber, *Angew. Chem.* **2007**, *119*, 8015; *Angew. Chem. Int. Ed.* **2007**, *46*, 7869; h) M. Stępień, B. Szysko, L. Latos-Grażyński, *J. Am. Chem. Soc.* **2010**, *132*, 3140.
- [2] a) M. G. P. M. S. Neves, R. M. Martins, A. C. Tomé, A. J. D. Silvestre, A. M. S. Silva, V. Félix, M. G. B. Drew, J. A. S. Cavaleiro, *Chem. Commun.* **1999**, 385; b) J.-Y. Shin, H. Furuta, K. Yoza, S. Igarashi, A. Osuka, *J. Am. Chem. Soc.* **2001**, *123*, 7190.
- [3] T. Koide, G. Kashiwazaki, M. Suzuki, K. Furukawa, M.-C. Yoon, S. Cho, D. Kim, A. Osuka, *Angew. Chem.* **2008**, *120*, 9807; *Angew. Chem. Int. Ed.* **2008**, *47*, 9661.
- [4] a) S. Shimizu, J.-Y. Shin, H. Furuta, R. Ismael, A. Osuka, *Angew. Chem.* **2003**, *115*, 82; *Angew. Chem. Int. Ed.* **2003**, *42*, 78; b) S. Shimizu, N. Aratani, A. Osuka, *Chem. Eur. J.* **2006**, *12*, 4909; c) T. Koide, K. Youfu, S. Saito, A. Osuka, *Chem. Commun.* **2009**, 6047; d) T. Higashino, A. Osuka, *Chem. Sci.* **2013**, *4*, 1087; e) T. Higashino, A. Osuka, *Chem. Asian J.* **2013**, *8*, 1994; f) G. Karthik, J. M. Lim, A. Srinivasan, C. H. Suresh, D. Kim, T. K. Chandrashekar, *Chem. Eur. J.* **2013**, *19*, 17011.
- [5] a) Z. S. Yoon, A. Osuka, D. Kim, *Nat. Chem.* **2009**, *1*, 113; b) Y. Tanaka, S. Saito, S. Mori, N. Aratani, H. Shinokubo, N. Shibata, Y. Higuchi, Z. S. Yoon, K. S. Kim, S. B. Noh, J. K. Park, D. Kim, A. Osuka, *Angew. Chem.* **2008**, *120*, 693; *Angew. Chem. Int. Ed.* **2008**, *47*, 681; c) J. Sankar, S. Mori, S. Saito, H. Rath, M. Suzuki, Y. Inokuma, H. Shinokubo, K. S. Kim, Z. S. Yoon, J.-Y. Shin, J. M. Lim, Y. Matsuzaki, O. Matsushita, A. Muranaka, N. Kobayashi, D. Kim, A. Osuka, *J. Am. Chem. Soc.* **2008**, *130*, 13568; d) S. Tokui, J.-Y. Shin, K. S. Kim, J. M. Lim, K. Youfu, S. Saito, D. Kim, A. Osuka, *J. Am. Chem. Soc.* **2009**, *131*, 7240; e) M. Inoue, A. Osuka, *Angew. Chem.* **2010**, *122*, 9678; *Angew. Chem. Int. Ed.* **2010**, *49*, 9488.
- [6] Y.-S. Xie, K. Yamaguchi, M. Toganoh, H. Uno, M. Suzuki, S. Mori, S. Saito, A. Osuka, H. Furuta, *Angew. Chem.* **2009**, *121*, 5604; *Angew. Chem. Int. Ed.* **2009**, *48*, 5496.
- [7] a) S. Mori, A. Osuka, *J. Am. Chem. Soc.* **2005**, *127*, 8030; b) S. Mori, K. S. Kim, Z. S. Yoon, S. B. Noh, D. Kim, A. Osuka, *J. Am. Chem. Soc.* **2007**, *129*, 11344; c) M. Suzuki, A. Osuka, *J. Am. Chem. Soc.* **2007**, *129*, 464; d) M.-C. Yoon, S. Cho, M. Suzuki, A. Osuka, D. Kim, *J. Am. Chem. Soc.* **2009**, *131*, 7360; e) T. Higashino, J. M. Lim, T. Miura, S. Saito, J.-Y. Shin, D. Kim, A. Osuka, *Angew. Chem.* **2010**, *122*, 5070; *Angew. Chem. Int. Ed.* **2010**, *49*, 4950; f) H. Mori, Y. M. Sung, B. S. Lee, D. Kim, A. Osuka, *Angew. Chem.* **2012**, *124*, 12627; *Angew. Chem. Int. Ed.* **2012**, *51*, 12459.
- [8] M. Ishida, S.-J. Kim, C. Preihls, K. Ohkubo, J. M. Lim, B. S. Lee, J. S. Park, V. M. Lynch, V. V. Roznyatovskiy, T. Sarma, P. K. Panda, C.-H. Lee, S. Fukuzumi, D. Kim, J. L. Sessler, *Nat. Chem.* **2013**, *5*, 15.
- [9] a) S. Saito, J.-Y. Shin, J. M. Lim, K. S. Kim, D. Kim, A. Osuka, *Angew. Chem.* **2008**, *120*, 9803; *Angew. Chem. Int. Ed.* **2008**, *47*, 9657; b) J. M. Lim, J.-Y. Shin, Y. Tanaka, S. Saito, A. Osuka, D. Kim, *J. Am. Chem. Soc.* **2010**, *132*, 3105.
- [10] J. M. Lim, Z. S. Yoon, J.-Y. Shin, K. S. Kim, M.-C. Yoon, D. Kim, *Chem. Commun.* **2009**, 261.
- [11] *opp*-Tetraphenyl TPP-type porphyrins were already reported; see: a) J. Takeda, M. Sato, *Tetrahedron Lett.* **1994**, *35*, 3565; b) K. S. Chan, X. Zhou, M. T. Au, C. Y. Tam, *Tetrahedron* **1995**,



- 51, 3129; c) T. Nakanishi, K. Ohkubo, T. Kojima, S. Fukuzumi, *J. Am. Chem. Soc.* **2009**, *131*, 577.
- [12] During our attempts to obtain crystals of **10**, we isolated crystals with a triangular structure (see the Supporting Information). It is likely that the planar triangular hexaphyrins are more prone to stacking because of their planar structure, although the Möbius aromatic species is predominant in solution.
- [13] J.-Y. Shin, K. S. Kim, M.-C. Yoon, J. M. Lim, Z. S. Yoon, A. Osuka, D. Kim, *Chem. Soc. Rev.* **2010**, *39*, 2751.
- [14] One of the reviewers hypothesized that the methanesulfonate anion could act as a template to interact with the inward-pointing pyrrolic  $\beta$  protons. The distances between the oxygen atom of the methanesulfonate and the  $\beta$  protons are in the range of 2.58–2.76 Å for **4** and 2.67 Å for **11** (see the Supporting Information), suggesting favorable interactions in the triangular conformation.
-